

Onset of chaotic dynamics in a ball mill: Attractors merging and crisis induced intermittency

G. Manai

Università di Sassari, Dipartimento di Chimica, Via Vienna 2, I-07100 Sassari, Italy

F. Delogu

Università di Cagliari, Dipartimento di Ingegneria Chimica e Materiali, Piazza d'Armi, 09123 Cagliari, Italy

M. Rustici^{a)}

Università di Sassari, Dipartimento di Chimica, Via Vienna 2, I-07100 Sassari, Italy

(Received 21 September 2001; accepted 4 April 2002; published 18 July 2002)

In mechanical treatment carried out by ball milling, powder particles are subjected to repeated high-energy mechanical loads which induce heavy plastic deformations together with fracturing and cold-welding events. Owing to the continuous defect accumulation and interface renewal, both structural and chemical transformations occur. The nature and the rate of such transformations have been shown to depend on variables, such as impact velocity and collision frequency that depend, in turn, on the whole dynamics of the system. The characterization of the ball dynamics under different impact conditions is then to be considered a necessary step in order to gain a satisfactory control of the experimental set up. In this paper we investigate the motion of a ball in a milling device. Since the ball motion is governed by impulsive forces acting during each collision, no analytical expression for the complete ball trajectory can be obtained. In addition, mechanical systems exhibiting impacts are strongly nonlinear due to sudden changes of velocities at the instant of impact. Many different types of periodic and chaotic impact motions exist indeed even for simple systems with external periodic excitation forces. We present results of the analysis on the ball trajectory, obtained from a suitable numerical model, under growing degree of impact elasticity. A route to high dimensional chaos is obtained. Crisis and attractors merging are also found. © 2002 American Institute of Physics. [DOI: 10.1063/1.1484016]

Mechanochemistry is a branch of solid state physical chemistry dealing with the effects of mechanical energy storage, on the various properties of solid phases. In particular, mechanical energy is stored as excess energy in point and extended defects which induce local distortions of the ordered crystalline lattice determining deep modifications of the material properties as well as an increase of the chemical reactivity. In spite of its modern applications in materials science the capability of mechanical energy to induce chemical reactions is well recognized since ancient times.^{1,2} However, mechanochemistry was actually forgotten from the Middle Age onwards and only at the beginning of the 19th century W. Ostwald attracted the attention of the scientific community on it.³ Since then, the field of research on mechanochemical phenomena greatly developed. Starting from the end of the 1960s ball milling in particular became a popular procedure in powder metallurgy to synthesize materials with novel properties.⁴ After about 30 years, however, many initial expectations on possible industrial application of mechanical treatment have been disappointed.⁵ Different reasons have been invoked to explain such a situation.

Among the others, the scarce knowledge of the dynamics of ball milling devices, where milling bodies undergo a huge number of collisions during the processing. Under such conditions, indeed, any experimental measurement of the exact number of impacts and of the energy transferred to powders at collisions is greatly hindered. It becomes therefore impossible to relate the degree of structural evolution to the mechanical energy dissipated, maybe the most important macroscopic parameter used to characterize the yield of a mechanochemical reaction. Any information on the dynamics of milling bodies is then extremely valuable in order to quantitatively describe and rationalize the kinetic features of mechanically induced transformations. Preliminary investigations have already shown the possible occurrence of chaotic regimes during milling treatments.^{6,7} On the other hand, modeling results and experimental evidences demonstrate the occurrence of regular dynamical regimes allowing for the direct measurement of both the average collision frequency and impact energy.⁸ It becomes therefore important to study the transition from periodic to chaotic regimes in order to understand when and why transition takes place, so as to avoid it. Experimentalists are indeed mainly interested in periodic and regular regimes, which permit the full control of experimental parameters.

^{a)} Author to whom correspondence should be addressed. Electronic mail: rustici@ssmain.uniss.it

I. INTRODUCTION

Mechanochemical processing of powders by ball milling (BM) is an attracting synthetic route for the production of novel materials under nonequilibrium conditions.⁹ Usually carried out inside batch reactors, the mechanical treatment consists in a succession of impact events during which powder particles trapped between two colliding surfaces experience high rates of plastic deformation.¹⁰ The microstructural refinement and the defect storage processes increase the chemical reactivity to such a level that unusual behaviors arise with the formation of metastable structures.^{11–13} In a sense, the mechanical energy transferred by the grinding balls to the powders in the course of the processing plays a role similar to other forms of energy more commonly employed to induce physical and chemical transformations. However, the difficulty in quantifying and controlling the dynamical variables greatly hindered a better understanding of the complex phenomenology observed in a milling process.⁵ Mechanically induced phase transformations are in fact sensitive to the main parameters of the mechanical treatment. Not only the kinetic energy of the milling balls, determining the load exerted on the powder and then the degree of plastic deformation, but also the powder charge, the collision frequency and the mill geometry affect the feasibility and the rate of a given transformation.^{14–16} Further progress requires a reliable evaluation of the main parameters of the mechanical treatment and the detailed characterization of the dynamics of milling regimes.^{5,17} A contribution along these lines of inquiry has been recently given by Cocco and co-workers.^{18–20} They set up an experimental methodology providing the accurate measurement of both the collision frequency and the impact velocity for milling runs carried out with a single ball subject to nearly plastic collisions. In such a context, evidences of the occurrence of chaotic behaviors in the course of a ball milling process were also provided.²¹ The maximum Lyapunov exponent, having a positive value, was indeed evaluated from an experimentally determined temporal series of sequential collisions. In spite of the possible sources of experimental errors, the experimental findings clearly pointed out that the ball-vial dynamics is chaotic when elastic collisions take place.

The experimental findings concerning the collision energy and frequency, collected under nearly inelastic impact conditions, were then used as a guideline for the development of a computer modeling of the ball motion.²² The picture that emerged from the numerical simulation of the ball dynamics closely supports the experimental results, providing estimates in complete agreement with experimentally accessible quantities. Ascertained in this way, the reliability of the model and the numerical simulations have been used to explore the ball dynamics in conditions where a direct experimental evaluation of the milling parameters is not possible.

A preliminary investigation has been already performed under completely elastic impact conditions. Suitable nonlinear dynamics analysis proved that the ball undergoes an hyperchaotic dynamics characterized by three positive exponents in the Lyapunov spectrum.⁷

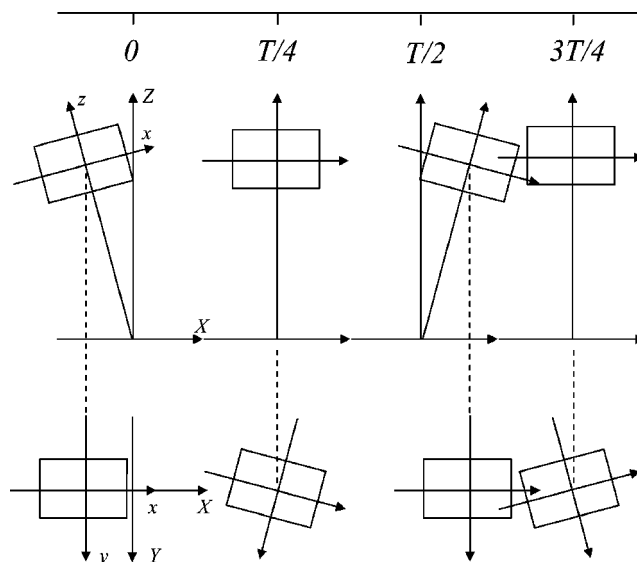


FIG. 1. Typical course of the Spex Mill. The vial motion is shown on the vertical ($X;Z$) and on the equatorial ($X;Y$) planes. The main component is a harmonic swing occurring over a shallow arc on the vertical plane. As shown in the lower graph, a synchronous additional movement makes the vial rotate around its barycenter on the ($X;Y$) plane.

In the present contribution, the analysis is pursued further and extended to all the possible impact conditions. The degree of impact elasticity is gradually changed and used as bifurcation parameter. The related ball dynamics changes correspondingly, showing more and more complex features as the impact conditions move from completely inelastic to completely elastic. In the following, the model of the ball-vial system is briefly outlined.

II. MODEL OUTLINE

The Spex Mixer/Mill model 8000 is the most diffuse BM device for mechanochemical activation of powders. A mechanical arm, mounted on an eccentric fulcrum and connected to an electrical engine, moves the vial, a cylindrical container 5.8 cm in height and 3.8 cm in diameter, along a complex three-dimensional course. The main component of the vial motion is an angular harmonic displacement on the vertical plane coupled with a synchronous rotation on the equatorial plane, as shown in Fig. 1. In a mill equipped with a suitable three-phase asynchronous motor, the vial can move with a frequency ranging between 14.6 and 22.5 Hz.¹⁹ The vial motion results from the combination of synchronous rototranslations with reference to a fixed frame of Cartesian axes. Two Cartesian reference systems, shown in Fig. 2, are used. The inertial one, of coordinates ($X;Y;Z$), is centered on the eccentric fulcrum, while the second, noninertial one of coordinates ($x;y;z$) has its origin coincident with the vial baricenter and moves with it. The periodic displacement of the mechanical arm on the vertical plane and the rotation on its own axis, R , are described by the following equations:

$$\theta = \theta_0 \cos(\omega t + \delta), \quad (1)$$

$$\alpha = \alpha_0 \sin(\omega t + \delta), \quad (2)$$

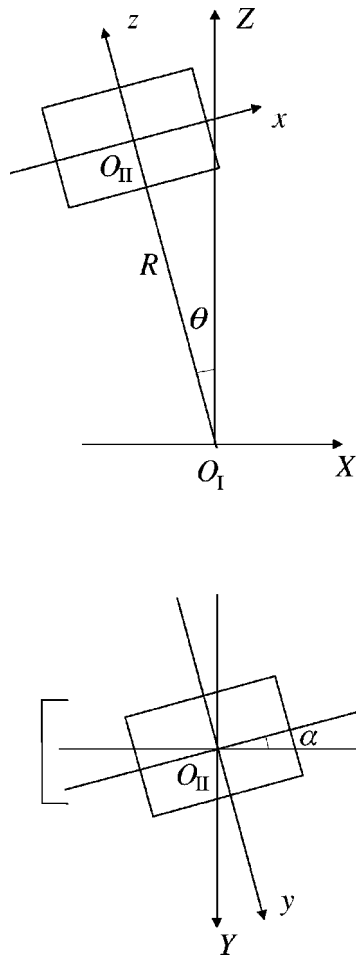


FIG. 2. Inertial (X;Y;Z) and noninertial (x;y;z) reference frames used to represent the vial motion. The vial, centered at the origin O_{II} of the latter, is also depicted. It oscillates on both the (X;Z) and (X;Y) planes with a $\pi/2$ phase difference. R represents the distance between the points O_I and O_{II} , corresponding to the origins of the two reference frames.

where θ_0 and α_0 are the amplitudes of the angular motions, $\omega = 2\pi\nu$, ν is the frequency of the motion, and δ is a phase factor dependent on the initial conditions. As evident from Fig. 2, the angles θ and α have a phase difference equal to $\pi/2$. The maximum angular amplitudes θ_0 and α_0 correspond to 15° , while the mechanical arm, R , is 10 cm long. The motion of any point of coordinates $(x;y;z)$ and $(X;Y;Z)$, in the noninertial and inertial reference systems, respectively, is described by the following sets of equations:

$$\begin{aligned} X &= (x \cos \alpha + y \sin \alpha) \cos \theta + (z + R) \sin \theta, \\ Y &= -x \sin \alpha + y \cos \alpha, \\ Z &= -(x \cos \alpha + y \sin \alpha) \sin \theta + (z + R) \cos \theta, \end{aligned} \tag{3}$$

and

$$\begin{aligned} x &= (X \cos \theta - Z \sin \theta) \cos \alpha - Y \sin \alpha, \\ y &= (X \cos \theta - Z \sin \theta) \sin \alpha + Y \cos \alpha, \\ z &= X \sin \theta + Z \cos \theta - R. \end{aligned} \tag{4}$$

Such equation sets allow for the reconstruction of the three-dimensional trajectory of any point of the vial. Together with

the geometrical constraints discussed below, the equations define the possible volume that the ball can explore in the course of its displacement inside the moving vial.

The effective volume available inside the vial for a ball with a diameter equal to 12.4 mm is defined by the following geometrical constraints on the noninertial ball center coordinates $(x_b; y_b; z_b)$:

$$-2.28 \leq x_b \leq 2.28 \text{ cm}, \quad (y_b^2 + z_b^2)^{1/2} \leq 1.28 \text{ cm}. \tag{5}$$

When an equality is satisfied, a collision occurs and the components of the ball velocity vector change. In particular, the component of the noninertial reference system velocity perpendicular to the surface of impact is reversed and scaled with a restitution coefficient f , according to the following equation:

$$v_f = -fv_i, \tag{6}$$

where v_i and v_f are, respectively, the initial and the final values of the velocity component. According to its usual definition, the restitution coefficient assumes values in the interval between 0 and 1. In the present work, the restitution coefficient f is gradually changed and the time series of noninertial ball coordinates, resulting from the numerical solution of the equations of motion, are analyzed in order to characterize the ball dynamic behavior. The restitution coefficient f is therefore used as bifurcation parameter. The equations of motion of vial and ball are numerically integrated with a time step δt equal to 10^{-5} s.

The equations of the first set above are integrated when the ball moves freely inside the vial in order to update the ball position. The position of the ball relative to the container walls is then checked with the second equation set. When conditions for impact between ball and container walls are satisfied, the first derivative of the equations is employed to determine the relative impact velocity.

The ball motion is obviously studied with reference to the vial displacement. Being ruled by the impulsive forces operating during the impact events, it only can be reproduced step-by-step by numerical calculations. Between two successive collisions, the ball motion is uniform rectilinear, since the gravity is neglected, and the course of the ball is described by the conventional Verlet algorithm:²³

$$\begin{aligned} r(t + \delta t) &= 2r(t) - r(t - \delta t) + a(t) \delta t^2, \\ v(t) &= [r(t + \delta t) - r(t - \delta t)] / 2\delta t, \end{aligned}$$

where r is the position vector, v is the velocity vector, a is the acceleration vector, t is the time, and δt the time step of integration. It is worth noting that, in the present case, acceleration is always absent since gravity is neglected. According to the simulation scheme adopted, when a collision takes place at a particular time step, the velocity is immediately inverted, its value being updated in the subsequent time step. It stems, therefore, that the collision event is limited to a single time step. Consequently, collision duration is equal to the time step adopted. Because of this, the value of the time step was chosen in order to provide a collision duration in rough agreement with data obtained from both the Hertzian theory of impact and experimental measurements.^{24,25} An

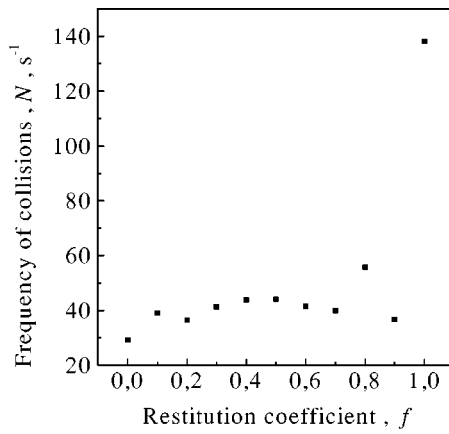


FIG. 3. Collision frequency N averaged as a function of restitution coefficient f .

improvement of the numerical model is certainly possible in order to reproduce in detail the dynamics of single impacts and valuable work has been already done in this direction.²⁶ Basic results on the system dynamical behavior, however, are not affected by the degree of accuracy with which a single impact event is simulated.

III. DATA ANALYSIS

For each value of the restitution coefficient f , a data set of six dynamical variables, consisting in the time series of ball coordinates $(x(t), y(t), z(t))$ and velocities $(\dot{x}(t), \dot{y}(t), \dot{z}(t))$, was generated by numerical solution of the equations of motion. Lowerscripts (b) are disregarded for the sake of simplicity. The length of the time series used for analyses is adapted to the main features of the ball dynamics. Longer series are generally needed to satisfactorily characterize the more complex regimes arising for values of the restitution coefficient larger than 0.3. Time series are, however, always longer than 10^9 points, corresponding to 10^4 s. Nonlinear dynamics analyses were performed on the data sets downsampled by a factor of 10. The sampling period effectively used is then equal to 10^{-4} s, still allowing for a satisfactory representation of the ball trajectory. Initial transients of variable length have also been observed. In each case, the system was allowed to settle down on the attractor and reach a stationary state and the initial data skipped. Analyses were then performed on data sets, suitably downsampled, and reduced, consisting of a minimum of 5×10^4 points.

IV. COMPUTATIONAL METHODS

A. Attractor reconstruction

The impossibility to make a continuous flow, i.e., a set of differential equations for the vial-ball system, induced us to reconstruct the attractor and to evaluate the Lyapunov exponents from the time series obtained by numerical modelling. The ball motion is governed by impulsive forces acting during each collision, and no analytical expression for the com-

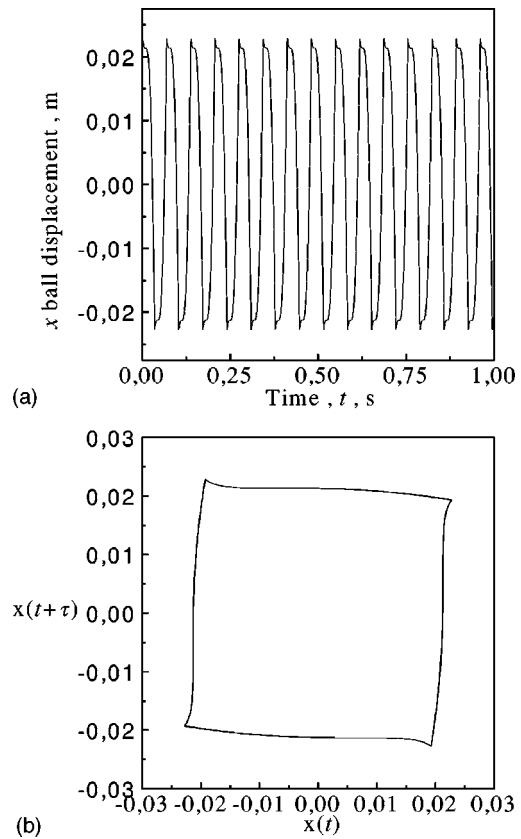


FIG. 4. Temporal series corresponding to the displacement along the non-inertial x axis for a restitution coefficient value equal to 0.13. Inversions at the maximum displacement points correspond to collisions occurring on the vial bases (a). Reconstructed attractor corresponding to a limit cycle (b).

plete ball trajectories can be obtained. However, the ball displacement as a function of the time can be followed step-by-step by numerical modeling.

Standard embedding techniques have been used to reconstruct the appropriate phase space for the ball dynamics, for each time series analyzed, from the original time series and its time delayed copies. Each time series can be regarded as a sequence of observations $\{s_n = s(\mathbf{x}_n)\}$ performed with some measurement function, where \mathbf{x}_n is defined in discrete time $t = n\Delta t$ by maps of the form

$$\mathbf{x}_{n+1} = \mathbf{f}(\mathbf{x}_n). \tag{7}$$

A delayed reconstruction in m dimensions is then formed by the vectors

$$\mathbf{s}_n = (s_{n-(m-1)\tau}, s_{n-(m-2)\tau}, \dots, s_{n-\tau}, s_n). \tag{8}$$

The number m of elements is referred to as the embedding dimension and the time τ is the so-called time delay, some integer multiple of the sampling period T_S . Since the number of embedding vectors is only $N - (m - 1)\tau$ when N scalar measurements are available, the dynamics is said to be embedded in an m -dimensional phase space. When a proper choice of the time delay and of the embedding dimension is made, the underlying assumption is that the invariants of the system dynamics are the same in both the actual and the reconstructed phase spaces.²⁷⁻³³ According to generally accepted procedures, the time delays (τ) have been calculated

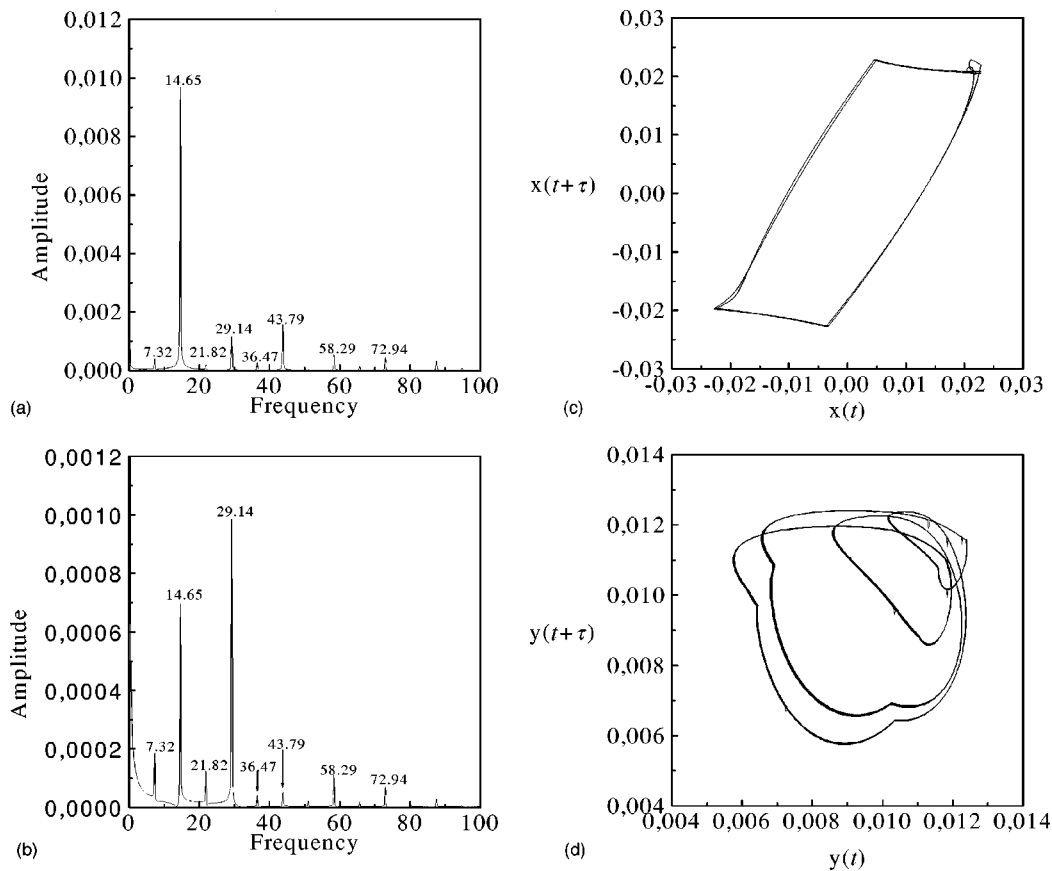


FIG. 5. Fast Fourier transform for the displacement along the noninertial x axis for a restitution coefficient value equal to 0.2 (a). Fast Fourier transform for the displacement along the noninertial y axis for a restitution coefficient value equal to 0.2 (b). Reconstructed attractor for x variable (c). Reconstructed attractor for y variable. In this case the fundamental frequency is equal to 29.14 Hz. The first period doubling has the same value of the fundamental frequency for the x axis. (d)

from the first minimum of the average mutual information function, which evaluates the amount of bits of information shared between two data sets over a range of time delays and provides adjacent delay coordinates with a minimum of redundancy.³⁴ The embedding dimension m , also critical to get a satisfactory reconstruction, has been computed from a global false-nearest-neighbors analysis evaluating the distance between neighboring trajectories at successively higher dimensions.³⁵ The uniqueness theorem about the solutions of autonomous differential equations guarantees, indeed, that no overlap of the orbit with itself is possible in the original phase space.^{27,28} False neighbors are therefore detected when trajectories overlapping in an m -dimensional space are distinguished in an m_{i+1} -dimensional one. As i increases, the total percentage of false neighbors decreases and the proper embedding dimension m is chosen where the percentage approaches zero. Under such circumstances, the attractor is unfolded and remains unfolded in higher dimensions. All the numerical calculations have been performed by using the TISEAN package.^{36,37}

B. Spectrum of Lyapunov exponents

It is well known that chaotic systems displays a sensitive dependence on initial conditions. Such a property is reflected on the time evolution of infinitesimally close trajectories which tend to diverge when the system dynamics is governed

by chaotic behaviors. The rate of divergence is measured by a characteristic quantity referred to as Lyapunov exponent. Actually, even in the case of a single dynamic variable time series, a spectrum of Lyapunov exponents (SLE) can be evaluated. The total number of exponents depends on the dimension of the phase space in which the dynamics is embedded. In the case of an n -dimensional phase space, n Lyapunov exponents ($\lambda_1 \geq \lambda_2 \geq \dots \geq \lambda_n$) are defined. Each one of the n Lyapunov exponents defined for a system with n degrees of freedom reflects the orbital stability along a proper direction. In particular, the system behavior will become more and more chaotic as the number of positive Lyapunov exponents increases. The largest one, λ_1 , determines the degree of chaoticity and then the timescale on which the dynamics becomes unpredictable. Various methods have been developed to evaluate the SLE.^{32,38-43} All of them consider the trajectory defined by the reconstructed attractor as a fiducial trajectory. The SLE calculation is based on the study of trajectories originating from points nearby the fiducial trajectory considered as distinct initial conditions along the fiducial trajectory itself. Therefore, an approximate reconstruction of the unknown dynamics \mathbf{f} is performed in the neighborhood of the fiducial trajectory. In the present paper, the Sano and Sawada algorithm^{36,37,41} has been used. Basically, it estimates the local Jacobians which rule the growth of infinitesimal perturbations. The routine employed

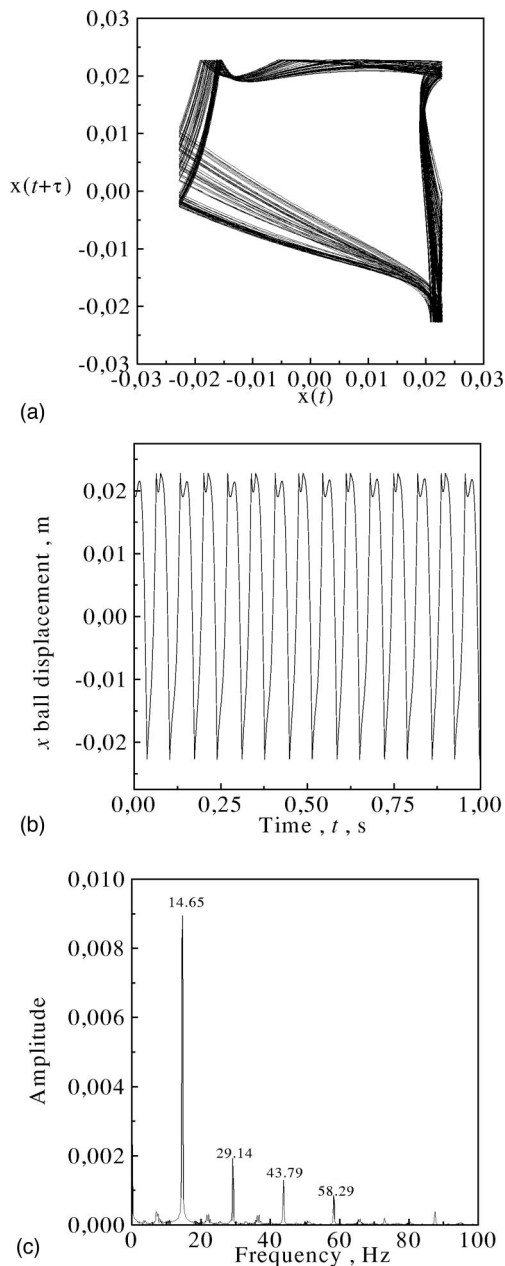


FIG. 6. Reconstructed attractor from the temporal series obtained from the x variable when the restitution coefficient is equal to 0.29 (a). Temporal series corresponding to the displacement along the noninertial x axis for a restitution coefficient value equal to 0.29 (b). Fast Fourier transform for the displacement along the noninertial x axis for a restitution coefficient value equal to 0.29 (c).

in TISEAN constructs a global nonlinear model and evaluates its local Jacobians by derivatives. The Jacobians are then multiplied to different vectors \mathbf{x}_k along the trajectory in the tangent space. The number of vectors \mathbf{x}_k equals the number of Lyapunov exponents in the SLE. The application, every few steps, of a Gram–Schmidt orthonormalization procedure gives the Lyapunov exponents in descending order.

V. RESULTS AND DISCUSSION

A ball inside the cylindrical mechanochemical reactor under operation is nothing but a particular kind of forced-and-damped oscillator. Forcing is assured by the motion of

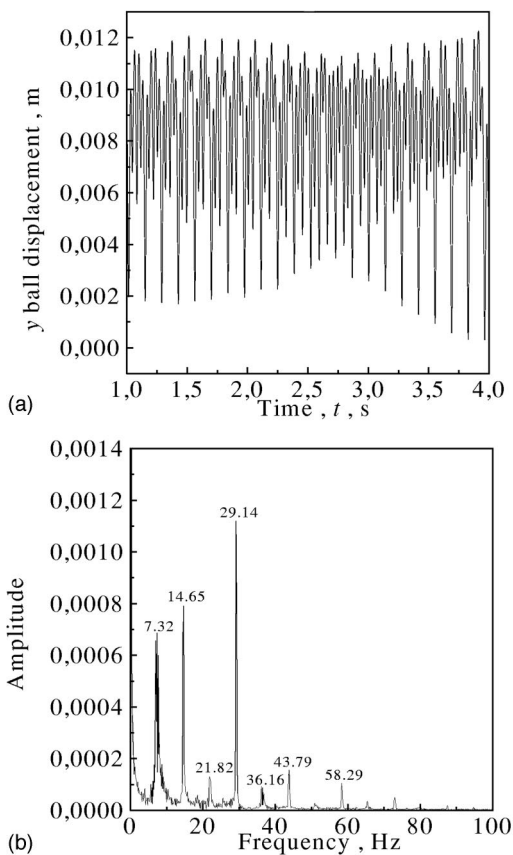


FIG. 7. Temporal series corresponding to the displacement along the noninertial y axis for a restitution coefficient value equal to 0.29 (a). Fast Fourier transform for the displacement along the noninertial y axis for a restitution coefficient value equal to 0.29 (b).

the reactor, which makes the ball travel in opposite directions along the vial axis, while damping is connected to the elasticity of impacts and, then, to the dissipation of kinetic energy taking place at each collision event. Keeping constant the frequency of the vial motion and changing the impact elasticity degree through a restitution coefficient corresponds, therefore, to change the “damping capacity” of the oscillator. The dynamics of such a system can be studied on different levels. On a “coarser” one, a simple quantity can be chosen as the reference parameter to characterize the dynamical behavior of the whole system. In the present work, the frequency, N , of impacts on the vial bases, i.e., the number of impacts that occurred on the vial bases in a second, has been chosen. An obvious increase in the impact frequency is expected at increasing the restitution coefficient f , and then the impact elasticity. The trend observed is, however, very different from a gradual, monotonous one. As shown in Fig. 3, the collision frequency N undergoes two sudden changes. Under inelastic impact conditions, the collision frequency is simply twice the milling frequency, equal to 14.58 Hz, pointing out a considerable regularity in the ball displacement. When the restitution coefficient f is 0.4, the collision frequency reaches a maximum. When f is 0.8 a sudden collision frequency jump occurs, and N moves from 39.78 to 55.7 Hz. When $0.9 \leq f \leq 1.0$ a second sudden jump occurs; the frequency reaches the value of 138.08 Hz. These

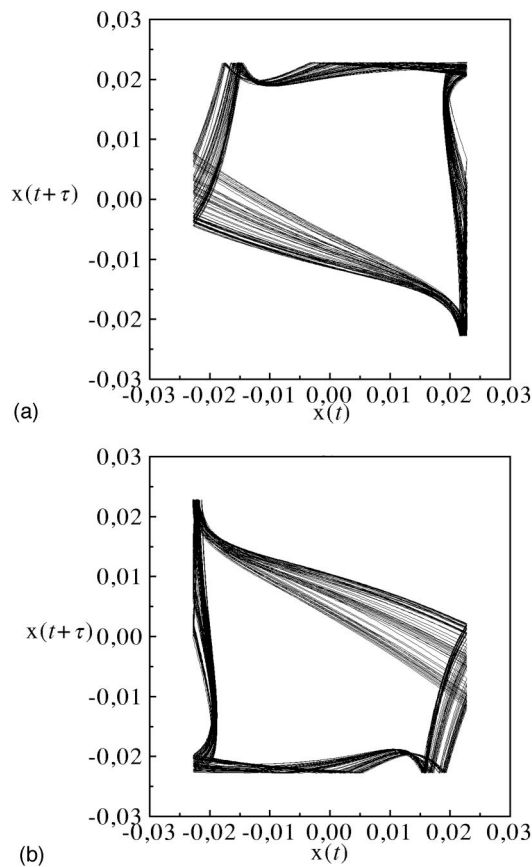


FIG. 8. Reconstructed attractor from the temporal series obtained from the x variable when the restitution coefficient is equal to 0.3 (a). Reconstructed attractor from the temporal series starting from different set of initial conditions obtained from the x variable when the restitution coefficient is equal to 0.3 (b).

results strongly support the occurrence of a disordered dynamics.⁸ On a “finer” level, nonlinear dynamics analytical tools have been used to fully characterize the ball dynamics and the nature of the transitions observed in the collision frequency at increasing the restitution coefficient f . Under inelastic impact conditions, i.e., at values of the restitution coefficient in the interval $0.0 \leq f \leq 0.28$, only periodic orbits are observed. Temporal series of the x coordinate are strictly similar to the periodic one, obtained for a restitution coefficient value equal to 0.13, reported in Fig. 4(a). Correspondingly, the attractor, shown in Fig. 4(b) and reconstructed by using a time delay of 1.71×10^{-2} s, is a limit cycle. As the value of the bifurcation parameter, f , increases in the interval between 0.0 and 0.28, the system is subjected to something similar to a period doubling sequence, as revealed by the appearance of frequencies from $\nu/2$ up to $\nu/2^2$. However, the added frequencies can not always be easily detected by analyzing the time series of the x coordinate only, since a strong dominant frequency is present. For example, the plot of the amplitude spectral density as a function of the frequency, reported in Fig. 5(a) for the x coordinate when the restitution coefficient is equal to 0.2, reveals only the $\nu/2$ frequencies. Nevertheless, the corresponding fast Fourier transform (FFT) of the y coordinate, quoted in Fig. 5(b), points out the occurrence of the $\nu/4$ frequencies also. The reconstructed attrac-

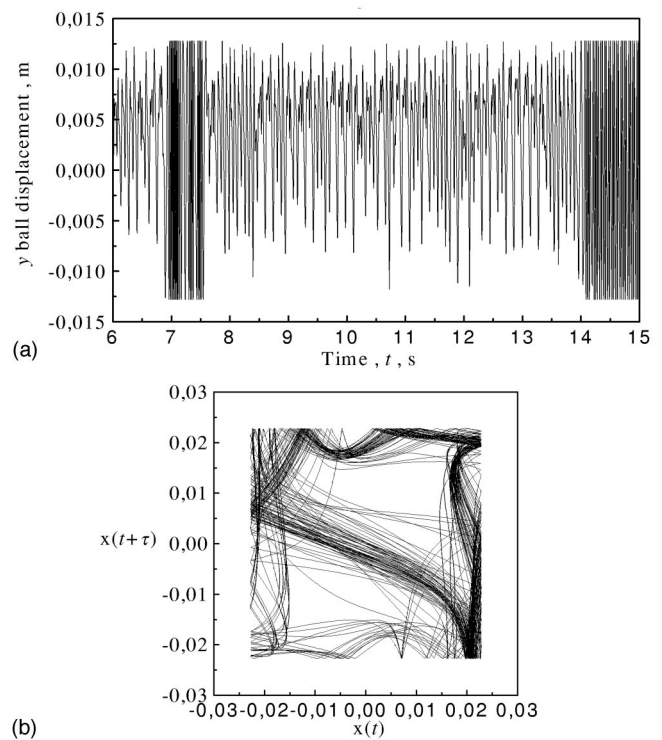


FIG. 9. Intermittency temporal series obtained from the y variable when the restitution coefficient is equal to 0.5 (a). Reconstructed attractor from the temporal series obtained from the x variable (b).

tors for both the x and y coordinates are shown in Figs. 5(c) and 5(d), respectively. The occurrence of the $\nu/4$ frequencies is particularly evident on Fig. 5(d). Actually, even if the frequencies observed in the range $0.2 \leq f \leq 0.29$ suggest a period-doubling cascade route to chaos,⁴⁴ it is not possible to exclude that the route to chaos consists, instead, in a scaling ratio sequence for a period adding sequence.⁴⁵ When the restitution coefficient reaches the value $f=0.29$ a chaotic behavior appears, characterized by a single positive Lyapunov exponent equal to 0.0029 s^{-1} . The attractor, reconstructed by the x coordinate, is shown Fig. 6(a). It is interesting to note that, at first sight, the system dynamics appears periodic. Both the temporal series and the FFT of the x coordinate, reported in Figs. 6(b) and 6(c), point out the occurrence of strictly periodic oscillations, dominated by a single fundamental frequency and its harmonics. Nevertheless, the analysis of the temporal series of the y and z coordinates reveals aperiodic patterns and broadband FFT spectra, although the fundamental frequencies are still the dominant ones, as evident from Figs. 7(a) and 7(b). The analysis of chaotic motions does not benefit much from power spectra, even if they are useful tools for the visualization of periodic and quasi-periodic phenomena and for their separation from chaotic time evolutions. In the present case, the strong dominant frequency on x coordinate hides the chaotic dynamics of the system. With reference to this, it is worth noticing the strength of the Takens theorem.³³ In fact, the reconstructed attractors from x and y coordinates both display the strangeness property typical of chaotic attractors, although the dynamics of the x coordinate seems to be periodic. Two positive Lyapunov exponents appear when the restitution

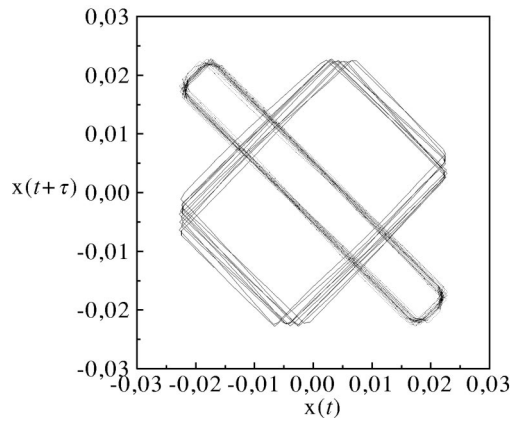


FIG. 10. Symmetric attractors obtained from the x variable starting from different sets of initial conditions ($f=1$ elastic condition).

coefficient assumes a value equal to 0.3, proving the establishment of a high-dimensional chaos. The reconstructed attractor is depicted in Fig. 8(a). As a matter of fact, the complexity of the dynamics inherent to this particular value of the bifurcation parameter is not evident from Fig. 8(a). Indeed, the symmetric properties of the system give rise to a different attractor that can be reconstructed starting from a different set of initial conditions. As evident from Fig. 8(b), the new attractor is perfectly symmetric to the one in Fig. 8(a). Increasing further the restitution coefficient leads to a crisis at the critical value ($f_c=0.4$).⁴⁶ In the present case, the sudden discontinuous change in the features of the chaotic attractor generally expected in a crisis scenario consists in the merging of the two attractors in Figs. 8(a) and 8(b) to form a new chaotic attractor. Before of the critical value, the basins of the two attractors are separated by a basin boundary. As f is increased, the two attractors enlarged and at the critical value f_c both of them simultaneously touch the basin boundary, colliding with saddle unstable orbits on it. For values $f > f_c$, an orbit will spend a long time in the region of one of the attractors existing separately when $f < f_c$. Then, the orbit will abruptly exit that region of phase space and will spend a long time in the region of the other attractor. Thus, for values $f > f_c$, the orbit intermittently switches be-

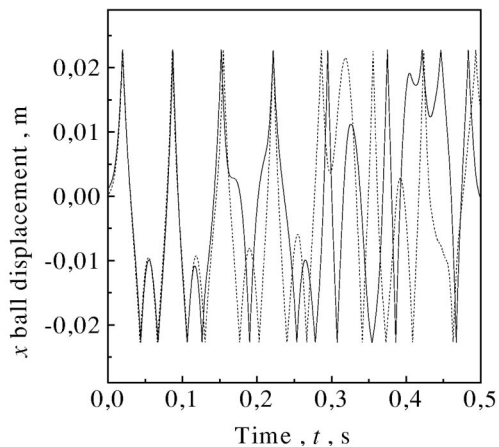


FIG. 11. Sensitive dependence on initial conditions.

tween two different regions of the phase space. Such a dynamic behavior is shown in Fig. 9(a) for a value of the restitution coefficient equal to $f=0.5$. The reconstructed attractor for the x coordinate is shown, instead, in Fig. 9(b). The intermittent behavior keeps until the restitution coefficient reaches the value $f=1$, corresponding to completely elastic impact conditions. As shown in Fig. 10, the attractor splits into two symmetric attractors. This attractor is responsible for a hyper-chaotic trajectory as already discussed in a previous paper.⁷ As evident from Fig. 11, the system dynamics is so sensitive that two orbits originating from very similar initial conditions become distinguishable after less than 0.15 s.

VI. CONCLUDING REMARKS

According to previous findings, the nonlinear dynamics analyses on the ball trajectories prove the complex nature of the ball dynamics in a milling device. When the restitution coefficient f is gradually changed in the interval between 0 and 1, the system dynamics correspondingly changes, undergoing subsequent transitions to chaos. Due to the symmetry of the system, two chaotic attractors are initially detectable in the phase space. Further increasing of the bifurcation parameter leads the system to hyperchaotic behavior characterized by an intermittent switching between two different basins in the phase space. The strong dependence of the ball motion on a bifurcation parameter such as the restitution coefficient underlines therefore the fundamental importance of the powder charge to control the collision elasticity and then the actual milling conditions. Work is in progress to deepen our insight into the detailed nature of intermittency and dynamical transitions. So far, we hope that our contribution could be useful to clarify the dynamics of the ball inside the Spex Mill and to favor further progress in the field of mechanochemistry.

¹Theofrasto di Ereso (IV sec B.C.) De Lapidibus.

²Anonymous (about 300 B.C.) De Natura Fossilium.

³W. Ostwald, *Handbuch Chemie*, I (Engleman, Leipzig, 1919), p. 70.

⁴J. S. Benjamin and T. Volin, *Metall. Trans.* **5**, 1929 (1974).

⁵B. B. Khina and F. H. Froes, *J. Metals* **48**, 36 (1996).

⁶P. H. Shingu, K. N. Ishihara, and A. Otsuki, *Mater. Sci. Forum* **179-181**, 5 (1995).

⁷C. Caravati, F. Delogu, G. Cocco, and M. Rustici, *Chaos* **9**, 219 (2000).

⁸F. Delogu, "Solid phase reactivity under mechanical processing condition. Structural evolution and transformation kinetics," Ph.D. thesis, Università degli studi di Sassari, 1999.

⁹C. Suryanarayana, *Prog. Mater. Sci.* **46**, 1 (2001).

¹⁰T. H. Courtney, *Mater. Trans., JIM* **36**, 110 (1995).

¹¹A. Y. Yermakov, Y. Y. Yurchikov, and V. A. Barinov, *Phys. Met. Metallogr.* **52**, 50 (1981).

¹²C. C. Koch, O. B. Cavin, C. G. McKamey, and J. O. Scarbrough, *Appl. Phys. Lett.* **43**, 1017 (1983).

¹³A. W. Weeber and H. Bakker, *Physica B* **153**, 93 (1988).

¹⁴G. Heinicke, *Tribochemistry* (Akademie-Verlag, Berlin, 1984), Chap. 5.

¹⁵Y. Chen, M. Bibole, R. Le Hazif, and G. Martin, *Phys. Rev. B* **48**, 14 (1993).

¹⁶H. Huang, M. P. Dallimore, J. Pan, and P. G. McCormick, *Mater. Sci. Eng., A* **241**, 38 (1998).

¹⁷Proceedings of the 1997 International Symposium on Mechanical Alloyed, Metastable and Nanocrystalline Materials, ISMANAM.

¹⁸F. Delogu, M. Monagheddu, G. Mulas, L. Schiffini, and G. Cocco, *Int. J. Non-Equilib. Process.* **11**, 235 (2000).

¹⁹F. Delogu, L. Schiffini, and G. Cocco, *Philos. Mag.* **A 81**(8), 1917 (2001).

- ²⁰F. Delogu, L. Schiffrini, and G. Cocco, *Mater. Sci. Forum* **360-362**, 337 (2001).
- ²¹M. Rustici, G. Mulas, and G. Cocco, *Mater. Sci. Forum* **225-227**, 243 (1996).
- ²²F. Delogu and G. Cocco, submitted.
- ²³M. P. Allen and D. J. Tildsley, *Computer Simulation of Liquids* (Oxford Science, Oxford, 1987).
- ²⁴E. H. Love, *A Treatise on the Mathematical Theory of Elasticity*, 4th ed. (Dover, New York, 1944), pp. 193–200.
- ²⁵S. P. Timoshenko and J. N. Goodier, *Theory of Elasticity* (McGraw-Hill, New York, 1970), pp. 409–422.
- ²⁶G. Manai, “Non linearità e caos nella dinamica di un gas granulare. Propagazione di reazioni combustive durante l’attivazione meccanochimica,” Tesi di Laurea in Chimica, Università degli studi di Sassari, 2000–2001.
- ²⁷H. Kantz and T. Schreiber, in *Nonlinear Time Series Analysis* (Cambridge University Press, Cambridge, 1997).
- ²⁸E. Ott, *Chaos in Dynamical Systems* (Cambridge University Press, New York, 1993).
- ²⁹D. S. Broomhead and G. P. King, *Physica D* **20**, 217 (1986).
- ³⁰H. D. I. Abarbanel, *Analysis of Observed Chaotic Data* (Springer-Verlag, New York, 1996).
- ³¹H. D. I. Abarbanel, R. Brown, J. J. Sidorowich, and L. S. Tsimring, *Rev. Mod. Phys.* **65**, 1331 (1993).
- ³²J. P. Eckmann and D. Ruelle, *Rev. Mod. Phys.* **57**, 617 (1985).
- ³³F. Takens, in *Dynamical Systems and Turbulence, Lecture Notes in Mathematics*, edited by D. A. Rand and L. S. Young (Springer-Verlag, Berlin, 1981), Vol. 898, p. 366.
- ³⁴A. M. Fraser and H. L. Swinney, *Phys. Rev. A* **33**, 1134 (1986).
- ³⁵M. B. Kennel, R. Brown, and H. D. I. Abarbanel, *Phys. Rev. A* **45**, 3403 (1992).
- ³⁶The TISEAN software package is publicly available at http://www.mpi-pks-dresden.mpg.de/~tisean/TISEAN_2.1/index.html. The distribution includes an online documentation system.
- ³⁷R. Hegger, H. Kantz, and T. Schreiber, *Chaos* **9**, 413 (1999).
- ³⁸J. M. Greene and J. S. Kim, *Physica D* **24**, 213 (1987).
- ³⁹J. P. Eckmann, S. O. Kamphorst, D. Ruelle, and S. Ciliberto, *Phys. Rev. A* **34**, 4971 (1986).
- ⁴⁰A. Wolf, J. B. Swift, H. L. Swinney, and J. A. Vastano, *Physica D* **16**, 285 (1985).
- ⁴¹M. Sano and Y. Sawada, *Phys. Rev. Lett.* **55**, 1082 (1985).
- ⁴²P. Bryant and R. Brown, *Phys. Rev. Lett.* **65**, 1523 (1990).
- ⁴³P. Bryant, R. Brown, and H. D. I. Abarbanel, *Phys. Rev. A* **43**, 2787 (1991).
- ⁴⁴M. J. Feigenbaum, *J. Stat. Phys.* **19**, 25 (1978).
- ⁴⁵Y. S. Fan and T. R. Chay, *Phys. Rev. E* **51**, 1012 (1995).
- ⁴⁶C. Grebogi, E. Ott, F. Romeiras, and J. A. Yorke, *Phys. Rev. A* **36**, 5365 (1987).